

Review Article

# Photocatalytic degradation of organic pollutants in the presence of selected transition metal nanoparticles: review

Tigabu Bekele Mekonnen\*

Department of Chemistry, Mekdela Amba University, Tuluawuliya, Ethiopia

## Abstract

Photocatalysis has attracted a lot of attention in recent years due to its potential in solving energy and environmental issues. Efficient light absorption and charge separation are two of the key factors for the exploration of high-performance photocatalytic systems, which are generally difficult to obtain from a single photocatalyst. The combination of various materials to form heterojunctions provides an effective way to better harvest solar energy and facilitate charge separation and transfer, thus enhancing photocatalytic activity and stability. This review concisely summarizes the recent development of visible light responsive heterojunctions, including the preparation and performance of semiconductor/semiconductor junctions and semiconductor/metal junctions and their mechanism for enhancing light harvesting and charge separation/transfer. In this regard, this review presents some unitary, binary and ternary CeO<sub>2</sub> photocatalysts used for the degradation of organic pollutants. We expect this review to provide the type of guidelines for readers to gain a clear picture of nanotechnology and the fabrication and application of different types of heterostructured photocatalysts.

## Introduction

Although dyes make our world beautiful, they bring us pollution. Color is the first contaminant to be recognized in wastewater and has to be removed before discharging it into water bodies or onto land. The colored wastewater of industrial effluents is unattractive because they account for significant concentrations of pollutants so they become the sources of increasingly acute complaints. Moreover, dyed (colored) wastewater usually consists of a number of contaminants including acids, bases, dissolved solids, toxic compounds and other colored materials. They can have acute or chronic effects on exposed organisms, which depend on the concentration of the dye and the exposure time. In addition to that, many dyes are considered to be toxic and even carcinogenic [1].

Dye-contaminated wastewater enters the environment through manufacturers and consumers such as the textile, leather, paper, printing, plastic and food industries usually in the form of a dispersion or a true solution and often in the presence of other organic compounds originating from operational processes [2]. The presence of small amounts of dyes in water (even < 1 ppm) is highly visible and it affects the pleasant appearance, causes significant loss in luminosity and any increase in the temperature will greatly deplete the

### More Information

\*Address for Correspondence: Tigabu Bekele Mekonnen, Department of Chemistry, Mekdela Amba University, Tuluawuliya, Ethiopia, Email: tgbekele19@gmail.com

Submitted: September 20, 2022

Approved: September 28, 2022

Published: September 29, 2022

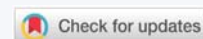
How to cite this article: Mekonnen TB. Photocatalytic degradation of organic pollutants in the presence of selected transition metal nanoparticles: review. J Plant Sci Phytopathol. 2022; 6: 115-125.

DOI: 10.29328/journal.jpssp.1001084

Copyright License: © 2022 Mekonnen TB. This is an open access article distributed under the Creative Commons Attribution License, which permits unrestricted use, distribution, and reproduction in any medium, provided the original work is properly cited.

Keywords: Nanotechnology; Nanoparticle; Ceria; Transition metals; Heterogeneous catalysis; Heterojunction; Doping; Coupling

Abbreviations: AOPs: Advanced Oxidation Process; BET: Brunauer-Emmett-Teller; CB: Conduction Band; e-CB: Electron in the Conduction Band; Eg: Bandgap Energy; h+VB: Hole in the Valance Band; MB: Methyl Blue; MO: Methyl Orange; NHE: Hydrogen Electrode Scale; RhB: Rhodamine Blue; TMs: Transition Metal; UV: Ultra Violet; UV/Vis: Ultra Violet and Visible light; VB: Valance Band



dissolved oxygen concentration in wastewater. This results in subsequent alteration of the aquatic ecosystem [3]. Thus, the presence of dye materials greatly influences the quality of water and the removal of this kind of pollutant is of prime importance [4].

Conventional dye removal methods, including physical, chemical, and biological processes, have been used intensively as a solution to the problem. But these methods have disadvantages such as impacts on health, high cost and difficulty in recycling. It is also a problem because these dye compounds in wastewater ordinarily contain one or several benzene rings and cannot be decomposed easily in chemical and biological processes. Moreover, most of the dyes are found to be resistant to processes as they are designed to resist chemical and photochemical degradation [5].

Advanced oxidation processes (AOPs) are efficient methods to remove organic contamination that is not

degradable by means of biological processes. AOPs are a set of processes involving the production of very reactive oxygen species able to destroy a wide range of organic compounds and bacteria cells [6,7]. In addition to these, AOPs rely on the in-situ production of highly reactive hydroxyl radicals ( $\bullet\text{OH}$ ). These reactive species are the strongest oxidants that can be applied in water and can virtually oxidize any compound present in the water matrix, thus  $\bullet\text{OH}$  reacts unselectively once formed and contaminants will be quickly and efficiently fragmented and converted into  $\text{CO}_2$  and  $\text{H}_2\text{O}$  [7,8]. In water, AOPs have the ability to destroy organic pollutants and furthermore, these processes are successful in inactivating bacteria, viruses, etc. Photocatalysis is the most relevant concept under advanced oxidation processes and it is the acceleration of a photoreaction in the presence of a catalyst. In catalyzed photolysis, light is absorbed by an adsorbed substrate or photocatalyst. In photogenerated catalysis, the photocatalytic activity depends on the ability of the catalyst to create electron-hole pairs, which generate free radicals (hydroxyl radicals:  $\bullet\text{OH}$ ) able to undergo secondary reactions.

## Nanomaterials

Nanocomposites are materials with at least one dimension in the nanometer range ( $1 \text{ nm} = 10^{-9} \text{ m}$ ). Nowadays, nanomaterials are of great interest from a research point of view, because the properties of the materials change drastically when the particle size reaches the nanometer range. As the size of the material becomes smaller, the band gap becomes larger thereby changing the optical and electrical properties of the material and making the material suitable for newer applications and devices. Further, the use of nanoparticles exhibits higher photocatalytic activity than their bulk counterparts by increasing their surface area and porosity [9].

Nanocomposite materials have emerged as suitable to overcome the limitations of micro and monolithic while posing preparation related to the control of elemental compositions and stoichiometry nanocluster phase. They are to be the materials of the 21<sup>st</sup> century in the view of possessing design uniqueness and property combinations that are not found in conventional composites. It has been reported that the changes in particle properties can be observed when the particle size is less than a particular level, called, the critical size [10]. As the dimensions reach the nanometer level, interactions at phase interfaces become largely improved, and this is important to enhance material properties. Now, several researchers have focused on metal oxide Nanoparticles and their composites for their high BET surface areas and fast kinetics when subjected to the treatment of organic pollutants in water and air. A general understanding of these properties and applications is very important.

Nano-particles of semiconductors have great potential for water purification catalysis and redox-active media due to their large surfaces, and their size and shape dependent on optical, electronic and catalytic properties [11]. Environmental

pollution has an influence on human survival and development. Nano-particles are of interest because of their high reactivity due to the large surface area-to-volume ratio. It was observed that nano-materials displayed significantly different properties at nanometer sizes as compared to the properties of the same material in bulk and that the properties of the materials are size and shape-dependent in the nanoscale range [12]. The large surface area of small-sized particles is expected to be beneficial for photocatalytic reactions that mostly occur on the surface of the catalysts [13].

## Nanocomposites and heterojunctions

The heterojunction is defined as the interface between two different semiconductors with an unequal band structure. Typically, there are three types of conventional semiconductor heterojunctions; namely (i) straddling type, (ii) staggered type and (iii) those with a broken gap. In type-I (straddling type heterojunctions), the energy band gap of semiconductor A is wider than B, (as shown in Figure 1), resulting in the accumulation of the charge carriers on the semiconductor with a smaller band gap. Since both electrons and holes are accumulated on the same semiconductor, the recombination of charge carriers is still possible. In type-II (staggered type) heterojunction, the valence and CBs of semiconductor A are higher and lower than those of B. This results in the spatial separation of charge carriers, which prevents the recombination of electrons and holes. The type-III heterojunction (with a broken gap) is the same as the staggered type except that the staggering gap becomes so wide that electron-hole migration is not possible. Therefore, the separation cannot occur [14].

Besides conventional heterojunctions, many other forms of heterojunctions have also been studied. These include p-n heterojunction, surface heterojunction, direct Z-scheme heterojunction and semiconductor/graphene heterojunction. A p-n junction improves the photocatalytic performance by providing an additional electric field. This is achieved by combining n-type and p-type semiconductors. On the other hand, a surface heterojunction involves creating different crystal facets on the exposed surface of a semiconductor [15]. Although these heterojunctions tend to enhance the electron-hole separation, they also reduce the redox ability of the photocatalyst. In order to overcome this problem, a Z-scheme heterojunction has been employed to maximize the redox potential of the heterojunction systems. The Z-scheme photocatalytic system consists of two different semiconductors

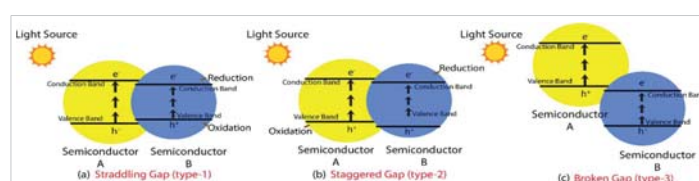


Figure 1: Types of conventional heterojunction (a) straddling gap; (b) staggered gap; (c) broken Gap [14].



and an acceptor/donor pair. The two semiconductors are not in physical contact, instead, the migration of the photogenerated holes takes place through the acceptor/donor pair [14].

### Properties of some selected nanoparticles

**Properties of TiO<sub>2</sub> nanoparticles:** The physical and chemical properties of Titania (titanium dioxide, TiO<sub>2</sub>) have been intensively studied for decades [16,17]. As a relatively inexpensive semiconductor material with nontoxicity, long-term stability, and chemical inertness in aqueous solutions [18], TiO<sub>2</sub> shows great prospects as a photocatalyst, in particular, for the degradation of organic pollutants in aqueous solutions. The earliest work of Titania photocatalysis was reported in 1921 by Renz, where it was found that Titania turned from white to a dark color under sunlight illumination in the presence of organic compounds such as glycerol. Photocatalytic activity of TiO<sub>2</sub> was also demonstrated by Fujishima and Honda who used TiO<sub>2</sub> for water splitting, an important process for solar energy conversion [19].

Nevertheless, the photocatalytic efficiency of TiO<sub>2</sub> alone is generally very low. This is primarily attributed to its wide band gap (~3.2 eV in anatase phase and ~3.0 eV in rutile phase) such that TiO<sub>2</sub> only absorbs lights in the UV region and thus it is challenging for practical applications with lights in the visible range as the source of excitation energy. Furthermore, the high recombination rate of the photo-generated electron/hole pairs also limits the efficiency of TiO<sub>2</sub>-based photocatalysts. Therefore, substantial efforts have been devoted to engineering the TiO<sub>2</sub> crystalline and morphological structures for the improvement of photocatalytic activity. For instance, one-dimensional TiO<sub>2</sub> nanostructures, such as nanowires, nanotubes and nanobelts, have attracted significant attention because of their relatively large specific surface areas that may lead to a marked improvement in photocatalytic activity [20,21]. In addition, doping of transition metals and their oxides or salts onto the surface of the TiO<sub>2</sub> photocatalysts has also been exploited as an effective route to improve the efficiency and range of photo absorption and hence the photocatalytic performance [22].

**Properties of ZnO nanoparticles:** Zinc oxide (ZnO) is an important industrial material because it is an inorganic and semiconducting material with inherent properties that share the same structure as Wurtzite [23]. The ZnO nano-composite has attracted interest because of its optical properties. These particles are transparent to visible light, but they absorb UV light. ZnO has attracted intensive research efforts for its unique properties and versatile applications in transparent electronics, chemical sensors and spin electronics. ZnO is soluble in acids and alkalis but not nearly soluble in water. In nature, it occurs as a mineral called zincate. Crystalline zinc oxides exhibit piezoelectric behavior. When heated with carbon, the oxides convert into zinc. It has a variety of applications, including medical, chemical and biosensors. Due

to its high isoelectric points (9.5), biocompatibility, and fast electron transfer interest, attention has recently been focused on the applications of ZnO in bio-sensing. ZnO is reactive toward both acids and bases, so it is considered an amphoteric oxide. Nano-sized ZnO has been widely used as a catalyst [24], gas sensor [25], active filler for rubber and plastic, UV absorber in cosmetics, and antiviral agent in coating and has more potential application in building functional electronic devices with special architecture and distinctive optoelectronic properties [26]. It exhibits direct and wide band gaps, strong sensitivity of the surface to the presence of adsorbed species, and large excitation band energy. A partial list of the above properties distinguishes it from other semiconductors or oxides and makes it useful for applications.

ZnO can be considered a multifunctional material due to its physical and chemical properties [27], namely chemical stability, a broad range of radiation absorption and low toxicity [28,29]. ZnO is an n-type semiconductor having an energy band gap value of about 3.3 eV (in bulk). As a photocatalyst, ZnO has relatively low photodegradation efficiency, mainly because of its large band gap and fast internal recombination of photogenerated electron-hole pairs and the photo corrosion phenomenon, which can influence the degradation effect of organic pollutants [30,31]. In order to improve the ZnO photocatalytic properties, many attempts have been made by means of doping [32], loading noble metals [33], adding other semiconductor Nanoparticles [34,35], etc.

**Properties of CeO<sub>2</sub> nanoparticles:** Cerium oxide (CeO<sub>2</sub>) is a metal oxide semiconductor that has been of interest recently because CeO<sub>2</sub> is a semiconductor light absorber in the UV (=388 nm) and visible region. CeO<sub>2</sub> is one of the most efficient photocatalysts, with a band gap energy (E<sub>bg</sub>) of 3.2 eV [36]. It is one of the most important catalytic materials that can play multiple roles owing to its ability to release and uptake oxygen under catalytic reaction conditions with the preservation of its fluorite structure [37]. However, the catalytic efficiency of ceria may be reduced at elevated temperatures due to sintering and loss of surface area [38]. For example, thermal stability is a critical issue in determining the promoting and metal supporting functions of CeO<sub>2</sub> in its catalytic applications in the three-way catalytic processes. For this reason, significant efforts have been made by the industry in trying to find ways to improve thermal stability, either by alternative methods involving the synthesis of ceria or by modifying the different types of stabilizers involved [39].

**Properties of Ag<sub>3</sub>PO<sub>4</sub> nanoparticles:** In recent years, silver-based photocatalysts with sufficient charge separation ability under visible light have received increased attention. Among such, silver phosphate (Ag<sub>3</sub>PO<sub>4</sub>) has been supposed as a promising high-efficient semiconductor material in the research fields due to its visible light response towards photodegradation of organic pollutants and bacteriostatic properties [40]. Ag<sub>3</sub>PO<sub>4</sub>, a renowned narrow band gap

semiconductor (2.36 - 2.43 eV), has been demonstrated to be a promising visible-light-sensitive photocatalyst, which can achieve an extremely high quantum yield up to 90% for  $O_2$  evolution under visible light (420 nm) [41]. It has been reported that  $Ag_3PO_4$  exhibits higher photocatalytic activity under visible light than that of other photocatalysts mentioned in the literature; it has thus inspired great enthusiasm [42]. However, due to the high surface-to-volume ratio, nanostructure  $Ag_3PO_4$  in powder form tends to agglomerate and leads to a decrease in effective surface area, which in turn decreases photocatalytic efficiency. Therefore, most of the attempts have been focused on the fabrication of inorganic/ $Ag_3PO_4$  heterostructures by coupling with different semiconductor materials, such as  $Ag_3PO_4/CeO_2$  [43],  $Ag_3PO_4/TiO_2$  [44],  $Ag_3PO_4/ZnO$  [45], etc. But the fabrication of organic/ $Ag_3PO_4$  composites by combining with polymer nanofibers in a well-defined manner has been rarely studied.

**Properties of CdS nanoparticles:** Cadmium sulphide (CdS) is an II-VI semiconductor that is insoluble in water, but soluble in dilute mineral acids. It exhibits intrinsic n-type of conductivity caused by sulphur vacancies due to excess cadmium atoms [46]. CdS in bulk have band gap energy of 2.42eV at 300K with absorption maxima at 515 nm [47,48]. It can attain three types of crystal structures namely Wurtzite, zinc blend and high-pressure rock-salt phase. Among these, Wurtzite is the most stable of the three phases and can be easily synthesized.

CdS Nanoparticles have been of huge interest because of their potential technological applications in the field of solar cells, photo-electronic devices, sensors, cell imaging and photocatalysts. Photocatalysis is the process of charge separation due to the absorbance of light energy greater than or equal to the band gap of the semiconductor material. This charge separation creates electron-hole pairs which lead to the generation of free radicals in the system. These generated radicals are good oxidizers and degrade pollutants. It is an effective technique for a waste-water treatment containing organic dyes [49].

### Photocatalytic activities of selected nanocomposites

#### Photocatalytic activities of pristine $CeO_2$ nanoparticle:

Pristine  $CeO_2$  has some properties like Titania features such as wide band gap, nontoxicity and high stability. Since its unique 4f electron configuration,  $CeO_2$  has been frequently selected as a component to prepare complex oxides or as a dopant to improve titania-based catalysts' performances [50].

Pouretedal and Kadkhodaie studied the degradation efficiency of MB (20 mg/L) versus irradiation time in the absence and presence of  $CeO_2$  Nanoparticles (0.5 g/L) at a pH of 7 as shown in Figure 2 [51]. Degradation of the MB molecules occurred under UV-Vis irradiation in the absence of any photocatalyst but at a slow rate. Irradiation in the presence of  $CeO_2$  Nanoparticles leads to an increase in

degradation efficiency.  $CeO_2$  is a semiconducting material and the onset of absorption will be at wavelengths lower than 420 nm [52]. Therefore, radiation of wavelength less than 420 nm is suitable for the transfer of electrons from the valance band to the conductance band.

#### Photocatalytic activities of $CeO_2/Ag_3PO_4$ nanoparticle:

Song, et al. reported the photocatalytic activity of the as-prepared samples is evaluated by the photocatalytic decomposition of some typical pollutants under visible light irradiation as seen in Figure 3 [53]. It can be found that the pure  $CeO_2$  hardly shows photocatalytic activity under the visible light illumination for MB. After 18 min of visible-light irradiation, the pure  $Ag_3PO_4$  shows good photocatalytic performance, and its photocatalytic degradation efficiency of MB is about 76%. The  $CeO_2/Ag_3PO_4$  (1 wt.%) composite degrades a relatively high level of MB (88%), which is increased by 12% in comparison with the pure  $Ag_3PO_4$ . As  $Ag_3PO_4$  is combined with  $CeO_2$ , the photocatalytic activity has some improvement, which illustrates that the introduction of  $CeO_2$  is an effective method for the enhancement of photocatalytic performance of the pure  $Ag_3PO_4$ . The improvement of photocatalytic activity for  $CeO_2/Ag_3PO_4$  hybrid materials could be attributed to the heterojunction between  $CeO_2$  and  $Ag_3PO_4$ .

#### Photocatalytic activities of $CeO_2/TiO_2$ nanoparticles:

Tju and his coworkers also synthesized  $TiO_2/CeO_2$  and

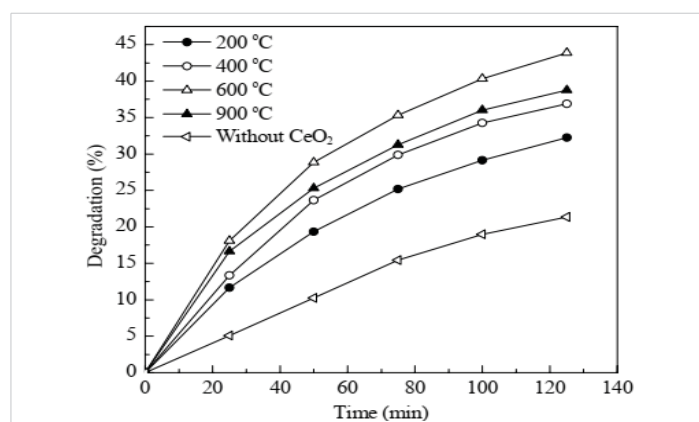


Figure 2: Degradation efficiency of MB (20 mg/L) at pH 7 catalyzed by  $CeO_2$  nanoparticles (0.5 g/L) calcined at different temperatures [51].

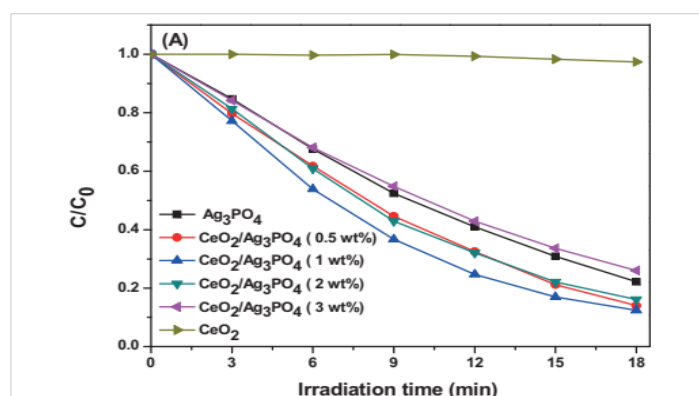


Figure 3: The degradation of MB under visible light irradiation with  $CeO_2/Ag_3PO_4$  composites [53].

evaluate the photocatalytic degradation performance of the photocatalyst over methyl blue (MB) dye under visible light irradiation [54]. To understand the catalytic activity exhibited by  $\text{TiO}_2/\text{CeO}_2$  nanocomposites, the correlation between the degradation of MB and the physical properties of the samples was proposed. According to BET measurement, in their study,  $\text{CeO}_2$  loading could increase the specific surface area of the samples. It can be seen the specific surface area of  $\text{CeO}_2/\text{TiO}_2$  has a larger surface area compared to  $\text{TiO}_2$  Nanoparticles. It has been reported that an increase in the specific surface area could increase the surface active site, which could increase the catalytic activity [55]. However, in their study, they obtain the  $\text{CeO}_2/\text{TiO}_2$  nanocomposites with the molar ratio of 1:0.5 exhibit the best catalytic activity in all catalytic experiments, these results indicated surface area alone could not yet determine the catalytic activity as indicated in Figure 4.

**ZnO/ $\text{CeO}_2$  nanoparticle to enhance photocatalytic performance:** Taufik and his coworkers also synthesized ZnO/ $\text{CeO}_2$  nanocomposites using the sol-gel method and tested the photocatalytic activity under visible light irradiation with methylene blue (MB) as a model of organic pollutants [56]. ZnO and  $\text{CeO}_2$  photocatalyst still has limitations due to the high rate of electron recombination and holes; moreover, they can only be activated using ultraviolet (UV) light irradiation [57]. To overcome these problems, Taufik and his coworker combining a ZnO semiconductor with another semiconductor ( $\text{CeO}_2$ ) have proven to increase the photocatalytic activity [58,59]. Cerium (IV) oxide ( $\text{CeO}_2$ ) is an n-type semiconductor that has been commonly used as a supporting photocatalyst to increase photocatalytic activity [60]. The coupled  $\text{CeO}_2$  semiconductor with ZnO is able to inhibit the electron recombination and hole rate through the process of electron and hole transfer from one semiconductor to the others [61]. The methylene blue degradation efficiency of the ZnO/ $\text{CeO}_2$  (1:0.3, 1:0.5, 1:1) nanocomposite samples under visible light irradiation are shown in Figure 5. Their findings show that the usage of ZnO/ $\text{CeO}_2$  nanocomposite with a molar ratio of 1:0.5 resulted in the best degradation ability under visible light irradiation.

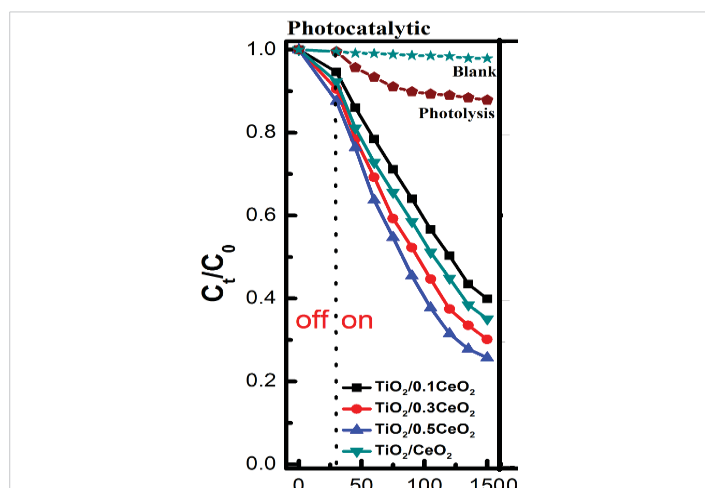


Figure 4: Photocatalytic activity with various samples [54].

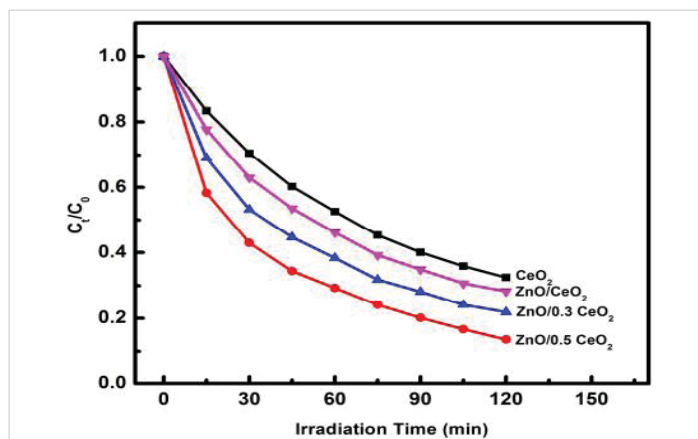


Figure 5: Photocatalytic activity of ZnO/ $\text{CeO}_2$  nanocomposites with different molar ratios [56].

The photocatalytic activities of the pristine ZnO and  $\text{CeO}_2/\text{ZnO}$  catalysts were also evaluated in terms of the degradation of methyl orange (MO) under a fluorescent lamp [62]. MO degradation was measured by observing the change in the adsorption spectra of MO at 464 nm, as shown in Figures 6a and b. Photocatalysts based on  $\text{CeO}_2/\text{ZnO}$  showed higher photocatalytic activity, which can degrade 94.06% of MO after 60 min. In contrast, the photocatalysts based on pristine ZnO can degrade 69.42% of MO. The results suggest an improvement of MO photocatalytic degradation due to an increase in Ce ion doping.

### Proposed photocatalytic degradation mechanism

A possible photocatalytic degradation mechanism of the  $\text{CeO}_2/\text{ZnO}$  catalysts is displayed in Figure 7. The band-edge positions of the conduction ( $E_{\text{CB}}$ ) and valence band ( $E_{\text{VB}}$ ) of metal-oxide semiconductors can be calculated using the equations [63]:

$$E_{\text{CB}} = X - E_{\text{c}} - 0.5 \times E_{\text{g}} \quad (1)$$

$$E_{\text{VB}} = E_{\text{g}} - E_{\text{CB}} \quad (2)$$

Where X is the electronegativity of ZnO and  $\text{CeO}_2$  (5.79 for ZnO and 5.56 eV for  $\text{CeO}_2$ ),  $E_{\text{c}}$  is the free electron energy on the hydrogen electrode scale (4.5 eV) and  $E_{\text{g}}$  is the band-gap energy (3.18 for ZnO and 3.00 eV for  $\text{CeO}_2$ ).

According to the conduction and valence band equations, the calculated  $E_{\text{CB}}$  and  $E_{\text{VB}}$  of ZnO were located at -0.30 and 2.88 eV. In contrast, the calculated  $E_{\text{CB}}$  and  $E_{\text{VB}}$  of  $\text{CeO}_2$  were located at -0.44 and 2.56 eV. A  $\text{CeO}_2/\text{ZnO}$  heterojunction forms due to the band-edge potentials between ZnO and  $\text{CeO}_2$ , which is beneficial for photocatalytic activity in terms of preventing charge recombination. Additionally, some  $\text{Ce}^{4+}$  ions may have drifted to the surface of the ZnO, which can promote more trapped electrons by the reaction  $\text{Ce}^{4+} + e^- \rightarrow \text{Ce}^{3+}$ . The product of this reaction can react with oxygen molecules to form superoxide radicals by the reaction  $\text{Ce}^{3+} + \text{O}_2 \rightarrow \text{Ce}^{4+} + \text{O}_2^{\cdot-}$ . The generated radicals (superoxide radicals and hydroxyl radicals) then degrade MO and produce oxidized organic products.

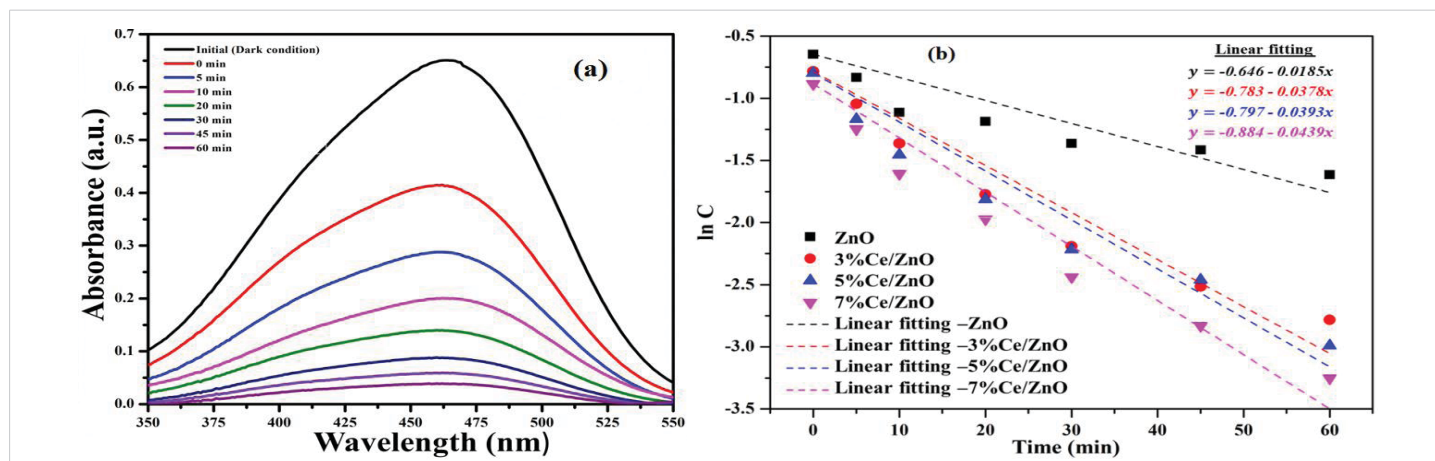


**Figure 6:** (a) Change in absorption spectra of the CeO<sub>2</sub>/ZnO catalysts (b) First-order kinetic adsorption curves during photodegradation of methyl orange [62].

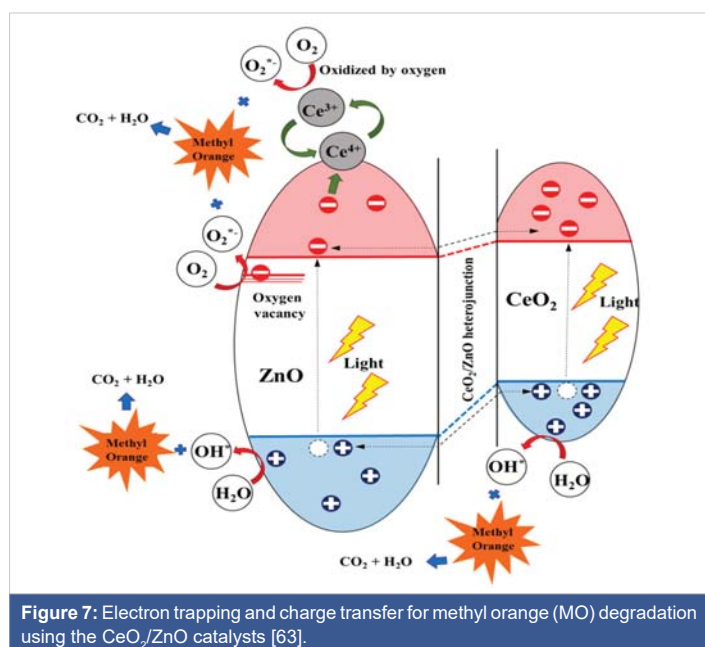


**Figure 7:** Electron trapping and charge transfer for methyl orange (MO) degradation using the CeO<sub>2</sub>/ZnO catalysts [63].

As a result, it can be seen that an increase in Ce ion doping can improve the photodegradation reaction rate compared with pristine ZnO. Finally, they draw a conclusion that Ce ion doping in CeO<sub>2</sub>/ZnO plays an important role in providing narrower optical energy band-gap tenability and defect generation, such as oxygen vacancies and oxygen interstitials, which controls photocatalytic activity. Additionally, the CeO<sub>2</sub>/ZnO heterojunction would provide a carrier pathway to separate photogenerated electron-hole pairs, obstructing charge recombination in CeO<sub>2</sub>/ZnO Nanoparticles.

**Photocatalytic activity of metal doped ceria nanoparticle:** Since the Ceria nanoparticle has a wide band gap energy (3.2eV) that limits further application. To overcome this problem doping with metal ions was chosen as it is believed to facilitate the Fenton reaction, which helps improve the photocatalytic activity by producing very powerful radicals as oxidizers [64,65]. The enhancement of photocatalytic activity for use as a catalyst in the visible region

is achieved by doping with transition metal ions such as iron to reduce the band gap energy level [66]. It has been reported that doping with multivalent transition-metal (TMs) cations was considered an effective method to inhibit the recombination of photogenerated carriers in semiconductors [67]. Theoretical investigation showed those metals have the greatest potential in permitting significant optical absorption in visible or even infrared solar light, through the combined effects of narrowed band gap and the introduction of intermediate bands within the forbidden gap [68,69]. Recently, there have been many reports on M-doped ceria oxide photoactivity under UV and visible light, such as Mn-CeO<sub>2</sub> [70], Fe-CeO<sub>2</sub> [71], Y-CeO<sub>2</sub> [72] and Sn-CeO<sub>2</sub> [73].

**Photocatalytic properties of mn-doped ceria nanoparticle:** Li and his coworkers obtained and compare pure and flower-like Mn-doped CeO<sub>2</sub> nanostructure by a simple one-step composite-hydroxide-mediated method [74]. The effective incorporation of Mn<sup>2+</sup> ions into CeO<sub>2</sub> crystalline lattices can greatly enhance the light photocatalytic performance. The UV/Vis spectral changes of Rhodamine blue (RhB) solution over 1% Mn-doped CeO<sub>2</sub> samples during the photodegradation, clearly show that the characteristic absorption peaks corresponding to RhB decrease rapidly as the exposure time increases, indicating the decomposition of RhB and the significant reduction in the RhB concentration. Figure 8a shows the results of RhB photodegradation over Mn-doped CeO<sub>2</sub> samples with different Mn doping concentrations.

After 210 min of irradiation, the photodegradation efficiencies of RhB were about 65, 40, and 30% for 1, 3, and 5% Mn-doped CeO<sub>2</sub> samples, respectively. It was evident that 1% Mn-doped CeO<sub>2</sub> samples exhibited excellent photocatalytic activities for RhB degradation. However, the photocatalytic performance of Mn-doped CeO<sub>2</sub> samples decreased with the increase of the Mn-doped amount. The results show that there was an optimal Mn doping concentration in CeO<sub>2</sub> samples for the ultraviolet light photocatalysis (1% Mn dopant). When the Mn doping concentration was further increased, the Mn

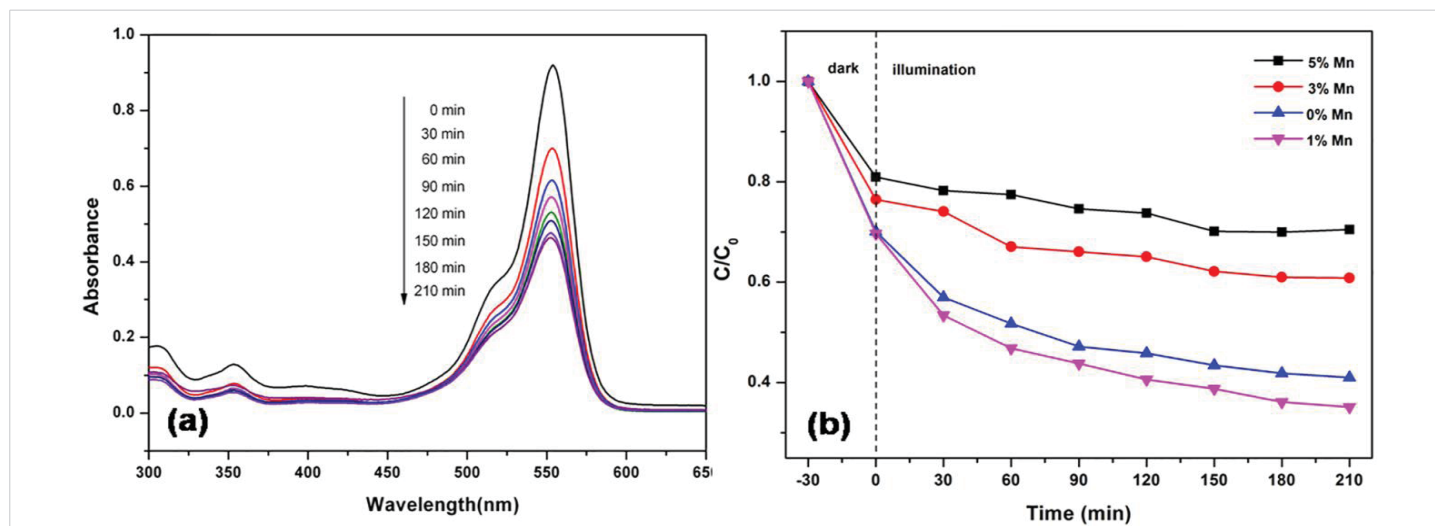


Figure 8: Degradation of RhB solutions over  $\text{CeO}_2$  and Mn-doped  $\text{CeO}_2$  with different Mn concentrations under ultraviolet light [74].

dopant sites could also act as efficient recombination centers with increased recombination rates due to the reduced average distance between trapped carriers [75]. The excess Mn dopant sites could greatly decrease the number of charge carriers and deteriorate the photocatalytic performance of doped  $\text{CeO}_2$  samples, as identified in Figure 8b.

**Photocatalytic properties of Fe-doped ceria nanoparticle:** Channei and his coworkers presented the decolorization of methyl orange (MO) using a Fe-doped  $\text{CeO}_2$  nanoparticle [71]. Their result clearly confirmed that iron-modified  $\text{CeO}_2$  films presented superior photocatalytic activity towards the degradation of MO in pH 5 conditions compared to undoped  $\text{CeO}_2$ , with 1.50 mol% Fe doping providing the most rapid dye degradation as indicated in Figure 9. BET analysis showed that the 1.50 mol% Fe-doped  $\text{CeO}_2$  film possessed the highest specific surface area, and hence more active sites are available for the MO degradation reaction [76].

### Proposed mechanism

Based on the optical band gap energy values the conduction band (CB) and valence band (VB) potentials of  $\text{CeO}_2$  can be calculated as:

$$E_{\text{CB}}(\text{CeO}_2) = \chi(\text{CeO}_2) - \{E_{\text{c}} - 1/2 E_{\text{g}}\} \quad (3)$$

$$E_{\text{VB}}(\text{CeO}_2) = E_{\text{g}} - E_{\text{cb}}(\text{CeO}_2) \quad (4)$$

Where  $\chi$  is the absolute electronegativity of the semiconductor ( $\chi$  is 5.56 eV for  $\text{CeO}_2$ ) [77].

EC is the scaling factor relating the hydrogen electrode scale (NHE) to the absolute vacuum scale (AVS) ( $\sim 4.5$  eV vs. AVS for 0 V vs. NHE) and  $E_{\text{g}}$  is the band gap energy of  $\text{CeO}_2$  (3.00 eV). The calculated CB and VB potentials of  $\text{CeO}_2$  are 20.44 and 2.56 eV, respectively.

It is proposed schematically in Figure 10 that the photo-generated electron-hole pairs are able to be separated into

trap states in the doped material. The presence of  $\text{Fe}^{3+}$ , may act as electron acceptor (from  $\text{Fe}^{3+}$  to  $\text{Fe}^{2+}$ ) and/or hole donor (from  $\text{Fe}^{3+}$  to  $\text{Fe}^{4+}$ ) to facilitate charge carrier localization and hence prolonged separation by trapping at energy levels close to the conduction or valence bands, respectively [78]. Therefore, the  $\text{Fe}^{3+}$  doping could be effective in producing materials that (1) delay electron-hole recombination, thereby increasing the lifetime of the electron-hole separation as confirmed in PL results and (2) support the charge carrier transfer to the catalyst surface [79].

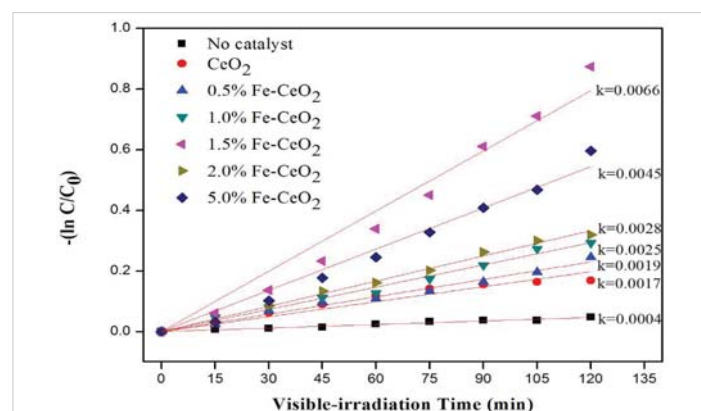


Figure 9: The kinetics plots for the pseudo-first-order reaction of MO decolorization at pH 5 [71].

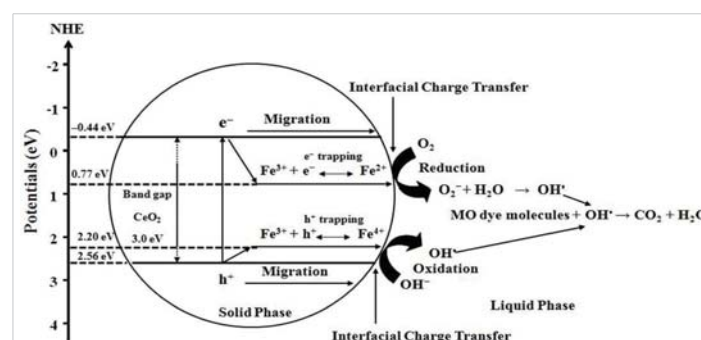


Figure 10: Proposed mechanism for the photoexcited electron-hole separation and transport processes at the Fe-doped  $\text{CeO}_2$  interface under visible light irradiation [71].

**Yttrium doped CeO<sub>2</sub> photocatalyst for photocatalytic application:** Since CeO<sub>2</sub> has a wide band gap energy semiconducting materials are restricted to degrade pollution under visible light. Doping Y-metal ion into cerium oxide reduces the bandgap and led to extended photocatalytic activity from UV to visible light, effectively preventing electron-hole recombination and leading to achieving photocatalytic activity under visible light [80].

Akbari-Fakhrabadi, et al. prepared pure and yttrium-doped CeO<sub>2</sub> nanocatalysts to degrade aqueous Rhodamine B (RhB) solution under visible light irradiation [72]. Figure 11 represents the time course degradation curve RhB for pure and yttrium-doped CeO<sub>2</sub> nanomaterials. It was observed that there is no degradation with the use of synthesized pure CeO<sub>2</sub> catalyst due to its large band gap [80]. During visible light irradiation, the wavelength of light is insufficient for a pure CeO<sub>2</sub> catalyst to make paired electrons and holes [80]. On the other hand, the yttrium-doped CeO<sub>2</sub> effectively degrades the RhB solution under visible light for 6 h because of the lower bandgap value which lies in the visible region, and this was confirmed from the UV/Visible reflectance spectrum. Also, visible light irradiated on the surface of yttrium doped CeO<sub>2</sub> catalyst effectively produces electrons and holes by reduction and oxidation process during the photocatalytic reaction due to the higher surface area of yttrium doped CeO<sub>2</sub> compared with pure CeO<sub>2</sub> [81,82]. These electrons and holes react with aqueous RhB solution and thus produce OH radicals which are capable of the effective degradation of RhB solution.

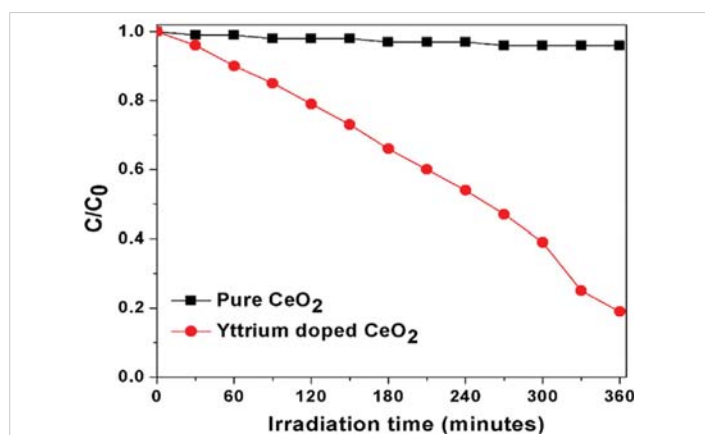


Figure 11: Time course degradation curve for 10 mg of prepared catalyst [72].

## Conclusion and future trends

Nanotechnology has proved a great achievement for controlling water purification challenges and making some future advancements. Nanomaterial approaches like nano sorbent, nanostructured catalytic membranes, etc. are very efficient, less time-consuming, less energy-consuming, and eco-friendly techniques, but all these methods are not cheap and they are not yet used for commercial purposes to purify the wastewater at a large scale. Nanomaterials show high efficiency due to their high rate of reaction. However, there

are still some weaknesses that must be negotiated. Up to now, no operational digital monitoring techniques exist that offer consistent real-time measurement facts on the superiority of Nanoparticles, which exist in small amounts in H<sub>2</sub>O. Furthermore, to reduce health risks, some research institutes and international research communities should prepare proper guidelines to overcome this issue. There is a great need to synthesize some modified nanomaterials which should be effective, have high efficiency, be easy to handle and be eco-friendly.

Semiconductor photocatalysis affords a potential solution to the problems of energy shortages and environmental pollution. However, the photo-efficiency of most single semiconductors is limited because of the rapid electron-hole recombination. Therefore, the development of efficient visible-light-driven photocatalysts is a major challenge in this field. Fortunately, the coupling of two or three semiconductors with different band gap values could improve the stability necessary for practical applications and could extend the energy range used for excitation. In particular, the fabrication of a p-n or n-n junction is believed to be the most effective because of the existence of an internal electric field. Moreover, the hybrid photocatalyst can benefit from synergistic effects such as enhanced light harvesting ability, efficient photogenerated electron-hole separation and improved photostability and thus, the photoactivity is remarkably improved.

Based on the literature data, it can be concluded that most of the photocatalytic investigations are focused on dye oxidation (methyl orange, Rhodamine B, methylene blue, malachite green, etc.) as the model degradation process of pollutants. The use of organic dyes as a model compound for photocatalytic decomposition reactions enables the feasible determination of photocatalytic activity, especially using spectrophotometric analysis.

From this point of view, there are still a few investigations into the photoactivity of composite photocatalysts that show enhanced photocatalytic activity for water splitting and organic degradation, except for dyes. Additionally, to better understand the properties of semiconductor composites and their role in photocatalytic processes, novel preparation methods need to be developed. Moreover, photocatalytic mechanisms and relationships among the structures forming the composites, surface and crystal properties should be thoroughly investigated and clarified.

The author recommends other researchers pay attention to advancing further research in this particular area by extending their modifications to improve the absorption of light.

We are looking for other binary and ternary or organic/inorganic doped to enhance the photocatalytic efficiency.

## Declaration of competing interest

This manuscript, entitled "Photocatalytic Degradation



of Organic Pollutants in the Presence of Selective Transition Metal Nanoparticles: Review," consists of 11 Figures. It has not been published previously and is not under consideration for publication elsewhere.

**Data availability statement:** The review manuscript data used to support the findings of this study are included within the article.

## References

- Rashed MN, El-Amin AA. Photocatalytic degradation of methyl orange in aqueous TiO<sub>2</sub> under different solar irradiation sources. *International Journal of Physical Sciences*. 2007; 2(3):073-081.
- Pelizzetti E, Serpone N eds. *Homogeneous and heterogeneous photocatalysis*. Springer Science & Business Media. 2012; 174
- Vakiti RK. *Hydro/solvothermal synthesis, structures and properties of metal-organic frameworks based on S-block metals*. 2012.
- Agarwal K. *Removal of Dyes Using Conventional and Advanced Adsorbents Advanced Adsorbents (Doctoral dissertation)*. 2013.
- Endashaw M, Girma T. Review on the removal of dyes by photodegradation using metal-organic frameworks under light irradiation. *Chemistry and Materials Research*. 2020; 12(1):14-21.
- Salih FM. Enhancement of solar inactivation of *Escherichia coli* by titanium dioxide photocatalytic oxidation. *J Appl Microbiol*. 2002;92(5):920-6. doi: 10.1046/j.1365-2672.2002.01601.x. PMID: 11972697.
- Pera-Titus M, García-Molina V, Baños MA, Giménez J, Esplugas S. Degradation of chlorophenols by means of advanced oxidation processes: a general review. *Applied Catalysis B: Environmental*. 2004; 47(4): 219-256.
- García-Montaño J, Pérez-Estrada L, Oller I, Maldonado MI, Torrades F, Peral J. Pilot plant scale reactive dyes degradation by solar photo-Fenton and biological processes. *Journal of Photochemistry and Photobiology A: Chemistry*. 2008; 195(2-3):205-214.
- Ozin GA, Cademartiri L. Nanochemistry: what is next? *Small*. 2009 Jun;5(11):1240-4. doi: 10.1002/smll.200900113. PMID: 19404992.
- Kausar A, Anwar S Graphite filler-based nanocomposites with thermoplastic polymers: a review. *Polymer-Plastics Technology and Engineering*. 2018; 57(6):565-580.
- Li F, Liang Z, Zheng X, Zhao W, Wu M, Wang Z. Toxicity of nano-TiO<sub>2</sub> on algae and the site of reactive oxygen species production. *Aquat Toxicol*. 2015 Jan;158:1-13. doi: 10.1016/j.aquatox.2014.10.014. Epub 2014 Nov 3. PMID: 25461740.
- Caruso RA, Antonietti M. Sol-gel nanocoating: an approach to the preparation of structured materials. *Chemistry of Materials*. 2001; 13(10):3272-3282.
- Seger B, Kamat PV. Electrocatalytically active graphene-platinum nanocomposites. Role of 2-D carbon support in PEM fuel cells. *The Journal of Physical Chemistry C*. 2009; 113(19):7990-7995.
- Low J, Yu J, Jaroniec M, Wageh S, Al-Ghamdi AA. Heterojunction Photocatalysts. *Adv Mater*. 2017 May;29(20). doi: 10.1002/adma.201601694. Epub 2017 Feb 21. PMID: 28220969.
- Gao S, Wang W, Ni Y, Lu C, Xu Z. Facet-dependent photocatalytic mechanisms of anatase TiO<sub>2</sub>: A new sight on the self-adjusted surface heterojunction. *Journal of Alloys and Compounds*. 2015; 647:981-988.
- Bilmes SA, Mandelbaum P, Alvarez F, Victoria NM. Surface and electronic structure of titanium dioxide photocatalysts. *The Journal of Physical Chemistry B*. 2000; 104(42):9851-9858.
- Chen X, Mao SS. Titanium dioxide nanomaterials: synthesis, properties, modifications, and applications. *Chem Rev*. 2007 Jul;107(7):2891-959. doi: 10.1021/cr0500535. Epub 2007 Jun 23. PMID: 17590053.
- Fujishima A, Rao TN, Tryk DA. Titanium dioxide photocatalysis. *Journal of Photochemistry and Photobiology C: Photochemistry Reviews*. 2000; 1(1):1-21.
- Fujishima A, Honda K. Electrochemical photolysis of water at a semiconductor electrode. *Nature*. 1972 Jul 7;238(5358):37-8. doi: 10.1038/238037a0. PMID: 12635268.
- Tan LK, Kumar MK, An WW, Gao H. Transparent, well-aligned TiO<sub>2</sub>(2) nanotube arrays with controllable dimensions on glass substrates for photocatalytic applications. *ACS Appl Mater Interfaces*. 2010 Feb;2(2):498-503. doi: 10.1021/am900726k. PMID: 20356197.
- Kang X, Chen S. Photocatalytic reduction of methylene blue by TiO<sub>2</sub> nanotube arrays: effects of TiO<sub>2</sub> crystalline phase. *Journal of Materials Science*. 2010; 45(10):2696-2702.
- Zhou W, Liu H, Wang J, Liu D, Du G, Cui J. Ag<sub>2</sub>O/TiO<sub>2</sub> nanobelts heterostructure with enhanced ultraviolet and visible photocatalytic activity. *ACS Appl Mater Interfaces*. 2010 Aug;2(8):2385-92. doi: 10.1021/am100394x. PMID: 20735112.
- González-Garnica M, Galdámez-Martínez A, Malagón F, Ramos CD, Santana G, Abolhassani R, Panda PK, Kaushik A, Mishra YK, Karthik TV, Dutt A. One dimensional Au-ZnO hybrid nanostructures based CO<sub>2</sub> detection: Growth mechanism and role of the seed layer on sensing performance. *Sensors and Actuators B: Chemical*. 2021; 337:129765.
- Chauhan MS, Kumar R, Umar A, Chauhan S, Kumar G, Faisal M, Hwang SW, Al-Hajry A. Utilization of ZnO nanocones for the photocatalytic degradation of acridine orange. *J Nanosci Nanotechnol*. 2011 May;11(5):4061-6. doi: 10.1166/jnn.2011.4166. PMID: 21780406.
- Pan JQ, Tian, Z. Grain size control and gas sensing properties of ZnO gas sensor. *Sensors and Actuators B: Chemical*. 2000; 66(1-3):277-279.
- Li AK, Wu WT, Kao CC, Chang RPH. Synthesis of monodispersed ZnO nanoparticles and their luminescent properties. *Key Engineering Materials*. 2003; 247:405-410.
- Suwanboon S, Amornpitoksuk P, Bangrak P, Random C. Physical and chemical properties of multifunctional ZnO nanostructures prepared by precipitation and hydrothermal methods. *Ceramics International*. 2014; 40(1):975-983.
- Kołodziejczak-Radzimska A, Jesionowski T. *Zinc Oxide-From Synthesis to Application: A Review*. Materials (Basel). 2014 Apr 9;7(4):2833-2881. doi: 10.3390/ma7042833. PMID: 28788596; PMCID: PMC5453364.
- Sirelkhatim A, Mahmud S, Seeni A, Kaus NHM, Ann LC, Bakhori SKM, Hasan H, Mohamad D. Review on Zinc Oxide Nanoparticles: Antibacterial Activity and Toxicity Mechanism. *Nanomicro Lett*. 2015;7(3):219-242. doi: 10.1007/s40820-015-0040-x. Epub 2015 Apr 19. PMID: 30464967; PMCID: PMC6223899.
- Xu F, Yuan Y, Han H, Wu D, Gao Z, Jiang K. Synthesis of ZnO/CdS hierarchical heterostructure with enhanced photocatalytic efficiency under nature sunlight. *Cryst Eng Comm*. 2012; 14(10):3615-3622.
- Han C, Yang MQ, Weng B, Xu YJ. Improving the photocatalytic activity and anti-photocorrosion of semiconductor ZnO by coupling with versatile carbon. *Phys Chem Chem Phys*. 2014 Aug 28;16(32):16891-903. doi: 10.1039/c4cp02189d. PMID: 25012572.
- Thi VHT, Lee BK. Effective photocatalytic degradation of paracetamol using La-doped ZnO photocatalyst under visible light irradiation. *Materials Research Bulletin*. 2017; 96:171-182.
- Sohrabnezhad S, Seifi A. The green synthesis of Ag/ZnO in montmorillonite with enhanced photocatalytic activity. *Applied Surface Science*. 2016; 386:33-40.
- Sang HX, Wang XT, Fan CC, Wang F. Enhanced photocatalytic H<sub>2</sub> production from glycerol solution over ZnO/ZnS core/shell nanorods



- prepared by a low temperature route. *International Journal of Hydrogen Energy*. 2012; 37(2):1348-1355.
35. Rao GT, Babu B, Stella RJ, Manjari VP, Reddy CV, Shim J, Ravikumar RVSSN. Synthesis and characterization of VO<sup>2+</sup> doped ZnO-CdS composite nanopowder. *Journal of Molecular Structure*. 2015; 1081:254-259.
  36. Toro RG, Malandrino G, Fragalà IL, Lo Nigro R, Losurdo M, Bruno G. Relationship between the nanostructures and the optical properties of CeO<sub>2</sub> thin films. *The Journal of Physical Chemistry B*. 2004; 108(42):16357-16364.
  37. Trovarelli A. *Catalysis by ceria and related materials*. World Scientific. 2002; 2.
  38. Craciun R, Daniell W, Knözinger H. The effect of CeO<sub>2</sub> structure on the activity of supported Pd catalysts used for methane steam reforming. *Applied Catalysis A: General*. 2002; 230(1-2):153-168.
  39. Kašpar J, Fornasiero P, Graziani M. Use of CeO<sub>2</sub>-based oxides in the three-way catalysis. *Catalysis Today*. 1999; 50(2):285-298.
  40. Liu JK, Luo CX, Wang JD, Yang XH, Zhong XH. Controlled synthesis of silver phosphate crystals with high photocatalytic activity and bacteriostatic activity. *Cryst Eng Comm*. 2012; 14(24):8714-8721.
  41. Yi Z, Ye J, Kikugawa N, Kako T, Ouyang S, Stuart-Williams H, Yang H, Cao J, Luo W, Li Z, Liu Y, Withers RL. An orthophosphate semiconductor with photooxidation properties under visible-light irradiation. *Nat Mater*. 2010 Jul;9(7):559-64. doi: 10.1038/nmat2780. Epub 2010 Jun 6. PMID: 20526323.
  42. Wang Z, Yin L, Zhang M, Zhou G, Fei H, Shi H, Dai H. Synthesis and characterization of Ag<sub>3</sub>PO<sub>4</sub>/multiwalled carbon nanotube composite photocatalyst with enhanced photocatalytic activity and stability under visible light. *Journal of Materials Science*. 2014; 49(4):1585-1593.
  43. Yang ZM, Huang GF, Huang WQ, Wei JM, Yan XG, Liu YY, Jiao C, Wan Z, Pan A. Novel Ag<sub>3</sub>PO<sub>4</sub>/CeO<sub>2</sub> composite with high efficiency and stability for photocatalytic applications. *Journal of Materials Chemistry A*. 2014; 2(6):1750-1756.
  44. Yao W, Zhang B, Huang C, Ma C, Song X, Xu Q. Synthesis and characterization of high efficiency and stable Ag<sub>3</sub>PO<sub>4</sub>/TiO<sub>2</sub> visible light photocatalyst for the degradation of methylene blue and rhodamine B solutions. *Journal of Materials Chemistry*. 2012; 22(9):4050-4055.
  45. Dong C, Wu KL, Li MR, Liu L, Wei XW. Synthesis of Ag<sub>3</sub>PO<sub>4</sub>-ZnO nanorod composites with high visible-light photocatalytic activity. *Catalysis Communications*. 2014; 46:32-35.
  46. Acharya KP. Photocurrent spectroscopy of CdS/plastic, CdS/glass, and ZnTe/GaAs hetero-pairs formed with pulsed-laser deposition (Doctoral dissertation, Bowling Green State University). 2009.
  47. Bhattacharya R, Saha S. Growth of CdS nanoparticles by chemical method and its characterization. *Pramana*. 2008; 71(1):187-192.
  48. Dumbrava A, Badea C, Prodan G, Ciupina V. Synthesis and characterization of cadmium sulfide obtained at room temperature. *Chalcogenide Lett*. 2010; 7(2):111-118.
  49. Bhadwal AS, Tripathi RM, Gupta RK, Kumar N, Singh RP, Shrivastav A. Biogenic synthesis and photocatalytic activity of CdS nanoparticles. *RSC Advances*. 2014; 4(19):9484-9490.
  50. Song S, Xu L, He Z, Chen J, Xiao X, Yan B. Mechanism of the photocatalytic degradation of C.I. Reactive Black 5 at pH 12.0 using SrTiO<sub>3</sub>/CeO<sub>2</sub> as the catalyst. *Environ Sci Technol*. 2007 Aug 15;41(16):5846-53. doi: 10.1021/es070224i. PMID: 17874796.
  51. Pouredal HR, Kadkhodaie A. Synthetic CeO<sub>2</sub> nanoparticle catalysis of methylene blue photodegradation: kinetics and mechanism. *Chinese Journal of Catalysis*. 2010; 31(11-12):1328-1334.
  52. Cullity BD. *Elements of X-ray Diffraction*. Addison-Wesley Publishing. 1956.
  53. Song Y, Zhao H, Chen Z, Wang W, Huang L, Xu H, Li H. The CeO<sub>2</sub>/Ag<sub>3</sub>PO<sub>4</sub> photocatalyst with stability and high photocatalytic activity under visible light irradiation. *Physica Status Solidi (a)*. 2016; 213(9):2356-2363.
  54. Tju H, Muzakki AT, Taufik A, Saleh R. Photo-, sono-, and sonophotocatalytic activity of metal oxide nanocomposites TiO<sub>2</sub>/CeO<sub>2</sub> for degradation of dye. In *AIP Conference Proceedings*. 2017; 1862:1; 030034.
  55. Wang X, Li S, Ma Y, Yu H, Yu J. H<sub>2</sub>WO<sub>4</sub>·H<sub>2</sub>O/Ag/AgCl composite nanoplates: a plasmonic Z-scheme visible-light photocatalyst. *The Journal of Physical Chemistry C*. 2011; 115(30):14648-14655.
  56. Taufik A, Shabrany H, Saleh R. Different heat treatment of CeO<sub>2</sub> nanoparticle composited with ZnO to enhance photocatalytic performance. In *IOP Conference Series: Materials Science and Engineering*. 2017; 188:1; 012038.
  57. Yin H, Yu K, Song C, Huang R, Zhu Z. Synthesis of Au-decorated V<sub>2</sub>O<sub>5</sub>@ZnO heteronanostructures and enhanced plasmonic photocatalytic activity. *ACS Appl Mater Interfaces*. 2014 Sep 10;6(17):14851-60. doi: 10.1021/am501549n. Epub 2014 Aug 27. PMID: 25140838.
  58. Shirzadi A, Nezamzadeh-Ejehie A. Enhanced photocatalytic activity of supported CuO-ZnO semiconductors towards the photodegradation of mefenamic acid aqueous solution as a semi real sample. *Journal of Molecular Catalysis A: Chemical*. 2016; 411:222-229.
  59. Mageshwari K, Nataraj D, Pal T, Sathyamoorthy R, Park J. Improved photocatalytic activity of ZnO coupled CuO nanocomposites synthesized by reflux condensation method. *Journal of Alloys and Compounds*. 2015; 625: 362-370.
  60. Contreras-García ME, García-Benjume ML, Macías-Andrés VI, Barajas-Ledesma E, Medina-Flores A, Espitia-Cabrera MI. Synergic effect of the TiO<sub>2</sub>-CeO<sub>2</sub> nanoconjugate system on the band-gap for visible light photocatalysis. *Materials Science and Engineering: B*. 2014; 183:78-85.
  61. Lamba R, Umar A, Mehta SK, Kansal SK. CeO<sub>2</sub>/ZnO hexagonal nanodisks: Efficient material for the degradation of direct blue 15 dye and its simulated dye bath effluent under solar light. *Journal of Alloys and Compounds*. 2015; 620: 67-73.
  62. Rodwihok C, Wongratanaphisan D, Tam TV, Choi WM, Hur SH, Chung JS. Cerium-oxide-nanoparticle-decorated zinc oxide with enhanced photocatalytic degradation of methyl orange. *Applied Sciences*. 2020; 10(5):1697.
  63. Khan MAM, Khan W, Ahamed M, Alhazaa AN. Microstructural properties and enhanced photocatalytic performance of Zn doped CeO<sub>2</sub> nanocrystals. *Sci Rep*. 2017 Oct 2;7(1):12560. doi: 10.1038/s41598-017-11074-7. PMID: 28970556; PMCID: PMC5624917.
  64. Channei D, Inceesungvorn B, Wetchakun N, Phanichphant S, Nakaruk A, Koshy P, Sorrell CC. Photocatalytic activity under visible light of Fe-doped CeO<sub>2</sub> nanoparticles synthesized by flame spray pyrolysis. *Ceramics International*. 2013; 39(3):3129-3134.
  65. An H, Li J, Zhou J, Li K, Zhu B, Huang W. Iron-coated TiO<sub>2</sub> nanotubes and their photocatalytic performance. *Journal of Materials Chemistry*. 2010; 20(3):603-610.
  66. Chung KH, Park DC. Water photolysis reaction on cerium oxide photocatalysts. *Catalysis Today*. 1996; 30(1-3):157-162.
  67. Chatterjee P, Mukherjee D, Sarkar A, Chakraborty AK. Mn-doped CeO<sub>2</sub>-CNT nanohybrid for removal of water soluble organic dyes. *Applied Nanoscience*. 2022; 1-13.
  68. Shao G. Electronic structures of manganese-doped rutile TiO<sub>2</sub> from first principles. *The Journal of Physical Chemistry C*. 2008; 112(47):18677-18685.
  69. Shao G. Red shift in manganese-and iron-doped TiO<sub>2</sub>: a DFT+ U analysis. *The Journal of Physical Chemistry C*. 2009; 113(16):6800-6808.



70. Li H, Zhou Y, Tu W, Ye J, Zou Z. State-of-the-art progress in diverse heterostructured photocatalysts toward promoting photocatalytic performance. *Advanced Functional Materials*. 2015; 25(7):998-1013.
71. Chaneei D, Inceesungvorn B, Wetchakun N, Ukritnukun S, Nattestad A, Chen J, Phanichphant S. Photocatalytic degradation of methyl orange by CeO<sub>2</sub> and Fe-doped CeO<sub>2</sub> films under visible light irradiation. *Sci Rep*. 2014 Aug 29;4:5757. doi: 10.1038/srep05757. PMID: 25169653; PMCID: PMC5385822.
72. Akbari-Fakhrabadi A, Saravanan R, Jamshidijam M, Mangalaraja RV, Gracia MA. Preparation of nanosized yttrium doped CeO<sub>2</sub> catalyst used for photocatalytic application. *Journal of Saudi Chemical Society*. 2015; 19(5):505-510.
73. Kumar KS, Jaya NV. Synthesis and Characterization of Pure and Sn-Doped CeO<sub>2</sub> Nanoparticles. *Asian Journal of Chemistry*. 2013; 25(11).
74. Li P, Zhang W, Zhang X, Wang Z, Wang X, Ran S, Lv Y. Synthesis, characterization, and photocatalytic properties of flower-like Mn-doped ceria. *Materials Research*. 2018; 21.
75. Choi W, Termin A, Hoffmann MR. The role of metal ion dopants in quantum-sized TiO<sub>2</sub>: correlation between photoreactivity and charge carrier recombination dynamics. *The Journal of Physical Chemistry*. 2002; 98(51):13669-13679.
76. Bangash FK, Alam S. Adsorption of acid blue 1 on activated carbon produced from the wood of *Ailanthus altissima*. *Brazilian Journal of Chemical Engineering*. 2009; 26:275-285.
77. Magesh G, Viswanathan B, Viswanath RP, Varadarajan TK. Photocatalytic behavior of CeO<sub>2</sub>-TiO<sub>2</sub> system for the degradation of methylene blue. 2009.
78. Masui T, Hirai H, Imanaka N, Adachi G, Sakata T, Mori H. Synthesis of cerium oxide nanoparticles by hydrothermal crystallization with citric acid. *Journal of Materials Science Letters*. 2002; 21(6):489-491.
79. Zhang Y, Jiang W, Wang C, Namavar F, Edmondson PD, Zhu Z, Gao F, Lian J, Weber WJ. Grain growth and phase stability of nanocrystalline cubic zirconia under ion irradiation. *Physical Review B*. 2010; 82(18):184105.
80. Saravanan R, Joicy S, Gupta VK, Narayanan V, Stephen A. Visible light induced degradation of methylene blue using CeO<sub>2</sub>/V<sub>2</sub>O<sub>5</sub> and CeO<sub>2</sub>/CuO catalysts. *Mater Sci Eng C Mater Biol Appl*. 2013 Dec 1;33(8):4725-31. doi: 10.1016/j.msec.2013.07.034. Epub 2013 Jul 30. PMID: 24094180.
81. Ansari SA, Khan MM, Ansari MO, Lee J, Cho MH. Visible light-driven photocatalytic and photoelectrochemical studies of Ag-SnO<sub>2</sub> nanocomposites synthesized using an electrochemically active biofilm. *RSC Advances*. 2014 4(49):26013-26021.
82. Ansari SA, Khan MM, Ansari MO, Cho MH. Gold nanoparticles-sensitized wide and narrow band gap TiO<sub>2</sub> for visible light applications: a comparative study. *New Journal of Chemistry*. 2015; 39(6):4708-4715.